Mon. Not. R. Astron. Soc. **000**, 000–000 (0000) Printed 5 February 2008 (MN LATEX style file v2.2)

Power spectrum of HI intensity fluctuations in DDO 210

Ayesha Begum[1⋆], Jayaram N. Chengalur[2] and Somnath Bharadwaj[3]†

[1]*National Centre for Radio Astrophysics, Post Bag 3, Ganeshkhind, Pune 411 007, India*
[2] *ATNF/CSIRO P. O. Box 76, Epping NSW 1710, Australia. On leave from NCRA/TIFR*
[3] *Department of Physics and Meteorology & Centre for Theoretical Studies , IIT Kharagpur, Pin: 721 302 , India.*

arXiv:astro-ph/0607367v1 17 Jul 2006

ABSTRACT

We measure the power spectrum of HI intensity fluctuations in the extremely faint ($\mathrm{M_B} \sim -10.9$) dwarf galaxy DDO 210 using a visibility based estimator that is well suited in very low signal to noise ratio regimes. DDO 210's HI power spectrum is well fit by a power law $\mathrm{P_{HI}}(U) = AU^{\alpha}$ with $\alpha = -2.75 \pm 0.45$ over the length-scales $80\,\mathrm{pc}$ to $500\,\mathrm{pc}$. We also find that the power spectrum does not change with an increase in the velocity channel width, indicating that the measured fluctuations correspond mainly to density fluctuations. However, Kolmogorov turbulence (with a velocity structure function spectral slope of 2/3) cannot be ruled out from the present observations. The value of the slope α is similar to that obtained in the Milkyway. In contrast to the Milkyway, DDO 210 has three orders of magnitude less HI, no spiral arms, and also no measurable ongoing star formation. The fact that the power spectrum slope is nonetheless similar in these two galaxies (and also similar to the values measured for the LMC and SMC) suggests that there is some universal, star formation independent, phenomenon responsible for producing fine scale structure in the gas.

Key words: galaxies: dwarf – galaxies: individual: DDO 210

1 INTRODUCTION

Evidence has been mounting in recent years that turbulence plays an important role in determining the physical conditions of the neutral ISM as well as for generating the hierarchy of structures seen in it (see Elmegreen & Scalo (2004) and Scalo & Elmegreen (2004) for recent reviews). Observational evidence includes the fact that the fluctuation power spectrum of a variety of tracers (HI 21cm emission intensity, HI 21cm optical depth, dust emission) is a scale free power law. The slope of the power law of HI 21cm emission and absorption in our own galaxy, HI 21cm emission from the LMC and SMC are all ~ -3 (Crovisier & Dickey (1983); Green (1993); Deshpande et al. (2000); Elmegreen et al. (2001); Stanimirovic et al. (1999)). Similarly, the HI distribution in several dwarf galaxies in the M81 group appears to be fractal (Westpfahl et al.(1999)), consistent with there being no preferred length scale. This scale free behaviour is characteristic of a turbulent medium; it is believed that the turbulence itself is driven by a combination energy input from spiral arms/bars and energy input from stellar sources (supernovae, stellar winds etc.).

Previous quantitative measurements of the HI emission power spectrum have been limited to the few cases (the Milkyway, LMC and SMC) where the HI signal is extremely strong. In this paper, we discuss the power spectrum of the fluctuations of HI 21cm emission intensity in DDO 210, the faintest ($\mathrm{M_B} \sim -10.9$) gas rich member of the local group. We use a visibility based estimator of the power spectrum; this is well suited to the current problem where the signal is buried deep in the noise. Visibility based methods also have the advantage of having well understood statistics, and being free of the uncertainties involved in gridding and image deconvolution. The rest of the paper is divided as follows. The power spectrum estimator that we use is discussed in detail in Sect. 2, the DDO 210 data presented in Sect. 3, while the results of applying the estimator to this data are shown in Sect. 4 and discussed in Sect. 5.

2 A VISIBILITY BASED POWER SPECTRUM ESTIMATOR

The power spectrum of HI emission $\mathrm{P_{HI}(u, v)}$ is the Fourier transform of the autocorrelation function $\xi(l - l', m - m')$ of the fluctuations in the HI brightness distribution $\delta I(l, m)$ i.e.

$$\xi(l - l', m - m') = \langle \delta I(l, m) \delta I(l', m') \rangle \tag{1}$$

and

$$\mathrm{P_{HI}}(u, v) = \int\int \xi(l, m)\, e^{-i2\pi(ul+vm)}\, dl\, dm \tag{2}$$

Here (l, m) refers to directions on the sky and (u, v) to inverse angular separations. The Fourier relation in Eqn. 2 assumes that the angular extent of the galaxy is small, a spherical harmonic decomposition would be needed otherwise. Further, it is assumed that the

⋆ E-mail:ayesha@ncra.tifr.res.in
† E-mail:somnathb@iitkgp.ac.in

statistical properties of the small scale fluctuations in the HI distribution are homogeneous and isotropic. The angular brackets denote an average across different positions and directions in the galaxy. It follows that the HI power spectrum $\mathrm{P_{HI}}(\vec{U})$ is a function of only the magnitude $U = \sqrt{u^2 + v^2}$.

Now, the complex visibility function measured by an interferometer is the Fourier transform of the brightness distribution,

$$V(u,v) = \int\int I(l,m)\, e^{-i2\pi(ul+vm)}\, dl\, dm\,. \tag{3}$$

It should be noted that (u, v) in Eqn. 3 refers to the projected baselines or antenna separations in units of the wavelength of observation. The Fourier relation in Eqn. 3 allows us to associate an inverse angular scale with every baseline (u, v) which we also denote using a two dimensional vector $\vec{U}$. Since the complex visibility measured by an radio interferometer is the Fourier transform of the HI intensity distribution, the squared modulus of the visibility is a direct estimator of the power spectrum,

$$\langle V(\vec{U}) V^*(\vec{U})\rangle = \mathrm{P_{HI}}(\vec{U}) \tag{4}$$

where $\langle ...\rangle$ now denotes an average over all possible orientations of the baselines $\vec{U}$.

This estimator has been used by both Crovisier & Dickey(1983) and Green(1993) to measure the power spectrum of HI fluctuations in our own galaxy. Eqn. 3 is an idealised one, in practice the interferometer response differs from the Fourier transform of the sky brightness both because it is modified by a window function and because there is added noise. We first consider the effect of the window function. In situations like in our own galaxy, where the HI emission fills the whole telescope beam, the window function is simply the primary beam of the telescope. In situations where the HI emission is from, for e.g., a distant galaxy whose angular extent is much smaller than the primary beam, the window function corresponds to the total extent of the HI emission. We will assume that, in general, the HI brightness distribution at any frequency ν can be written as

$$I_\nu(l,m) = W_\nu(l,m)\, [\bar{I}_\nu + \delta I_\nu(l,m)], \tag{5}$$

where W_ν(l,m) is the window function which characterises the large scale HI distribution in the galaxy at frequency ν, $\bar{I}_\nu$ is the mean HI brightness and $\delta I_\nu(l,m)$ characterises the small scale fluctuations. For a window function with angular extent $1/D$, we expect its Fourier transform, $\tilde{W}(\vec{U})$, to be sharply peaked at $\vec{U} = 0$ and to fall off rapidly for $\mid \vec{U} \mid \gg D$. Then, at long baselines, where we can ignore the contribution from $W_\nu(l,m)\, \bar{I}_\nu$, the square of the complex visibility is the power spectrum $P_{HI}(\vec{U})$ convolved with the square of the Fourier transform of the window function, i.e.

$$\langle V_\nu(\vec{U})\, V_\nu^*(\vec{U})\rangle = \tilde{W}_\nu^2(\vec{U}) \otimes P_{HI}(\vec{U})\,. \tag{6}$$

Both Crovisier & Dickey (1983) and Green(1993) ignored the window function in their analysis, which is justified at large baselines if $\tilde{W}_\nu^2(\vec{U})$ is sharply peaked at $\vec{U} = 0$ and decays much faster than $\mathrm{P_{HI}}(\vec{U})$.

We now look at the effect of measurement noise. The measured visibility can be written as $V_\nu(\vec{U}) = S_\nu(\vec{U}) + N_\nu$, where $S_\nu(\vec{U})$ is the HI signal and N_ν is the noise. We then have

$$\langle V_\nu(\vec{U})\, V_\nu^*(\vec{U})\rangle = \langle S_\nu(\vec{U}) S_\nu^*(\vec{U})\rangle + \langle N_\nu N_\nu^*\rangle \tag{7}$$

where we see that squaring the complex visibility makes the noise bias positive-definite. For HI emission from our own galaxy this noise bias is small compared to the signal. On the other hand, the noise bias can be orders of magnitude larger than the desired power spectrum in the case of faint external galaxies. In principle, one could estimate $\langle N_\nu N_\nu^*\rangle$ from a line free frequency channel and subtract it from $\langle V_\nu(\vec{U})\, V_\nu^*(\vec{U})\rangle$ for a channel with emission. However this requires that the noise statistics at different frequency channels be determined at an extremely high level of precision. Uncertainties in the bandpass response usually render such high levels of precision unachievable.

The problem of noise bias can be avoided by correlating the visibilities at two different baselines for which the noise is expected to be uncorrelated. The correlation between the visibilities measured on two slightly different baselines is:

$$\begin{aligned}\hat{\mathrm{P}}_{\mathrm{HI}}(\vec{U}, \Delta\vec{U}) &= \langle V_\nu(\vec{U})\, V_\nu^*(\vec{U} + \Delta\vec{U})\rangle \\ &= \int \mathrm{P_{HI}}(\vec{U}^{'})[\tilde{W}_\nu(\vec{U} - \vec{U}^{'}) \times \tilde{W}_\nu^*(\vec{U} + \Delta\vec{U} - \vec{U}^{'})]\, d^2\vec{U}^{'}\,,\end{aligned} \tag{8}$$

Since $\tilde{W}(\vec{U})$ falls off rapidly for $\mid \vec{U} \mid \gg D$, it then follows that the two shifted window functions in Eqn. 8 will have a substantial overlap only if $|\Delta\vec{U}| < D$. Thus visibilities at two different baselines will be correlated only as long as $|\Delta\vec{U}| < D$, and not beyond. In our analysis we restrict the difference in baselines to $|\Delta\vec{U}| \ll D$ so that $\tilde{W}_\nu(\vec{U} + \Delta\vec{U} - \vec{U}^{'}) \approx \tilde{W}_\nu(\vec{U} - \vec{U}^{'})$. The expected value of the visibility correlation now no longer depends on $\Delta\vec{U}$ allowing us to introduce the notation $\hat{\mathrm{P}}_{\mathrm{HI}}(\vec{U}) = \langle V_\nu(\vec{U})\, V_\nu^*(\vec{U} + \Delta\vec{U})$ and

$$\hat{\mathrm{P}}_{\mathrm{HI}}(\vec{U}) = \int \mathrm{P_{HI}}(\vec{U}^{'}) \mid \tilde{W}_\nu(\vec{U} - \vec{U}^{'}) \mid^2\, d^2\vec{U}^{'}\,, \tag{9}$$

We use the real part of the measured visibility correlation $\hat{\mathrm{P}}_{\mathrm{HI}}(\vec{U})$ as an estimator of the HI power spectrum $\mathrm{P_{HI}}(\vec{U})$. This is the sum of the HI signal and a system noise contribution. The latter is unbiased and has a zero mean, its variance being determined by the noise statistics of the individual visibilities. The imaginary part of $\hat{\mathrm{P}}_{\mathrm{HI}}(\vec{U})$ is noise dominated. There will be a very small contribution from the HI signal because the assumption that $\tilde{W}_\nu(\vec{U} + \Delta\vec{U} - \vec{U}^{'}) \approx \tilde{W}_\nu(\vec{U} - \vec{U}^{'})$ is not strictly valid. The requirement that the imaginary part of $\hat{\mathrm{P}}_{\mathrm{HI}}(\vec{U})$ should be small provides a self-consistency check and allows us to determine the range of validity of our formalism.

A further simplification is possible for our estimator if we assume that $\tilde{W}_\nu(\vec{U})$ decays much faster than variations in $\mathrm{P_{HI}}(\vec{U}^{'})$. Such an assumption is justified at large baselines $U \gg D$ if, for example, $\mathrm{P_{HI}}(\vec{U})$ is a power law. We then have

$$\hat{\mathrm{P}}_{\mathrm{HI}}(\vec{U}) = \mathrm{P_{HI}}(\vec{U}) \left[\int \mid \tilde{W}_\nu(\vec{U}^{'}) \mid^2\, d^2\vec{U}^{'}\right]. \tag{10}$$

where the quantity in square brackets [..] in Eqn. 10 is a constant. We note that while $\hat{\mathrm{P}}_{\mathrm{HI}}(\vec{U})$ directly estimates P_{HI} at large baselines $U \gg D$, it is necessary to account for the convolution (Eqn. 9) at small baselines $U \sim D$.

The utility of using visibility correlations as a statistical estimator of the HI power spectrum has been discussed previously by Bharadwaj & Sethi (2001) in the context of the large scale HI distribution at high redshifts. Visibility based statistical techniques are also of interest in the efforts to detect the epoch of reionization through interferometric HI observations (eg. Morales and Hewitt 2004;Bharadwaj and Ali 2005), and are also used in the analysis of interferometric observations of the CMBR (e.g. Hobson et al. (1995)).

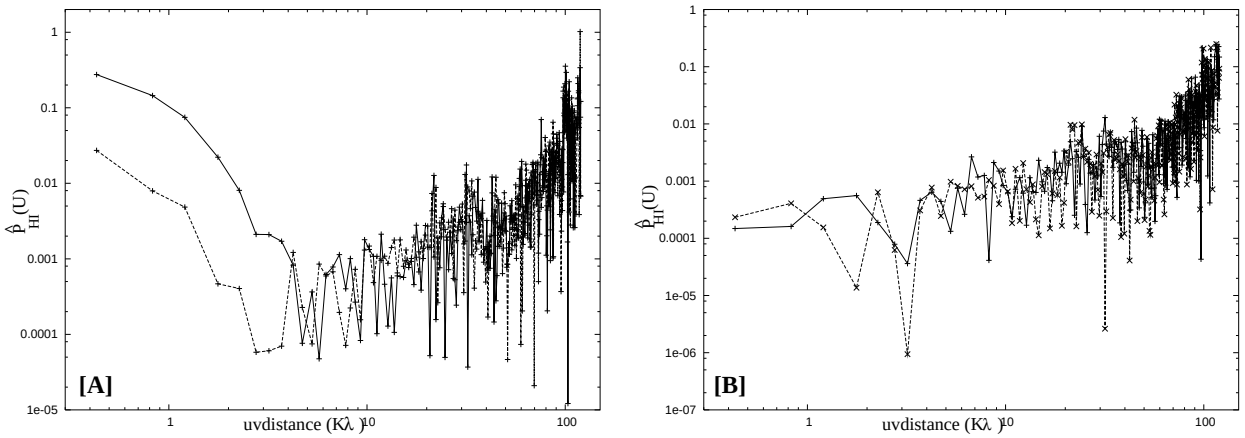

Figure 1. Absolute value of the real (solid line) and imaginary (dash line) parts of $\hat{\mathrm{P}}_{\mathrm{HI}}(\vec{U})$ plotted against the uv distance U for two different frequency channels of the GMRT data. **[A]** shows results for a channel with significant HI emission and **[B]** a channel with no HI emission, corresponding to heliocentric velocities of ~ -137 kms^{-1} and ~ -64 kms^{-1} respectively.

3 DATA

We apply the formalism developed above to interferometric observations of DDO 210. Since DDO 210 is relatively close (at a distance of 950$\pm$50 kpc; Lee et al. (1999)) the observations have good spatial resolution as well as comparatively good signal-to-noise ratio (SNR). Further, DDO 210 has been observed with both the Giant Metrewave Radio Telescope (GMRT) (Swarup et al. 1991) and in multiple configurations of the Very Large Array (VLA). A comparison of the power spectrum derived from these two independent data sets allows a robust check against systematic biases.

The GMRT data for DDO 210 have been discussed in detail in Begum & Chengalur (2004). We state the main observational results briefly below, the reader is referred to Begum & Chengalur (2004) for a more details. The HI emission from DDO 210 spanned the central 25 channels of the 128 channel spectral cube (with channel width $\sim$1.7 kms^{-1}). The HI disk of the galaxy is nearly face on. On large scales, the HI distribution is not axisymmetric; the integrated HI column-density contours are elongated towards the east and south. The maximum angular extent of the HI distribution for the galaxy is $D \sim 0.8$ kλ and does not change significantly in the central 10 frequency channels.

The VLA observations have been discussed in Young et al. (2003). For the current analysis we use raw data downloaded from the VLA archive and reanalysed by us.

4 RESULTS

We estimated $\hat{\mathrm{P}}_{\mathrm{HI}}(\vec{U})$ by correlating all the baselines within $\mid \Delta\vec{U} \mid \leqslant 0.2$ kλ. This value of $\Delta\vec{U}$ was chosen as a compromise between having sufficient visibility pairs to get a good SNR and ensuring that $\Delta\vec{U}$ itself remains small compared to $D \sim 0.8$ kλ. All self correlations (i.e. correlations of a visibility with itself) were excluded. The measured correlations were then binned in bins of 0.5 kλ width. Each frequency channel was treated separately, and the analysis was also carried out on the line free frequency channels as a check.

Fig. 1[A] shows the absolute value of the real and imaginary parts of $\hat{\mathrm{P}}_{\mathrm{HI}}(\vec{U})$ for a channel with HI emission, while Fig. 1[B] shows the same quantities for a channel with no emission. For the channel with emission, we find that at baselines less than ~ 5 kλ the real and imaginary parts of $\hat{\mathrm{P}}_{\mathrm{HI}}(\vec{U})$ are both positive, and the real part is substantially larger than the imaginary part. For the channel with no emission the real and imaginary parts are small and of comparable magnitude. This is in agreement with the cross-checks discussed in Sec. 2 for determining the reality of the signal. Henceforth, we will ignore the imaginary part of $\hat{\mathrm{P}}_{\mathrm{HI}}(\vec{U})$ and use the symbol $\hat{\mathrm{P}}_{\mathrm{HI}}(\vec{U})$ to refer to only the real part. Note that the apparent increase in the value of $\hat{\mathrm{P}}_{\mathrm{HI}}(\vec{U})$ seen at the longer baselines in Fig. 1[A]&[B] is because the noise is large in this range and we are plotting the absolute value of the estimator. The increase in noise is a consequence of the sparse sampling of the outer parts of the uv-plane.

Fig. 2 shows $\hat{\mathrm{P}}_{\mathrm{HI}}(\vec{U})$ determined separately from the GMRT and VLA data (for channels corresponding to very similar heliocentric velocity). The two estimates are in excellent agreement, which is a robust check on the reality of the signal. Fig. 2 also shows 1σ error bars for the estimated power spectrum. The errors were computed by including both the effect of having a fine number of estimates of the true spectrum ("cosmic variance") as well as having noisy visibility measurements. The first term was estimated as $\hat{\mathrm{P}}_{\mathrm{HI}}(\vec{U})\sqrt{D/2\pi U}$, while the second term was taken from the measured fluctuations of $\hat{\mathrm{P}}_{\mathrm{HI}}(\vec{U})$ for channels with no HI emission. The total 1σ error bars were determined by combining the two contributions in quadrature. At small baselines ($U \leqslant 5$ kλ), the first term dominates the error budget, while the noise on the measured visibilities dominates at large baselines.

If the observed power spectrum is due to turbulence in the interstellar medium, the slope of the derived power spectrum could change depending on the width of the frequency channel (Lazarian (1995)). Turbulence gives rise to fluctuations in both the density and velocity of the gas and both of these contribute to the observed intensity fluctuations. Lazarian & Pogosyan (2000) show that the statistical properties of the velocity and the density fluctuations can be disentangled if the slope of the observed power spectrum changes depending on whether the intensity is averaged over a velocity range that is large ("thick slices") or small ("thin slices") compared to the turbulent velocity dispersion. For DDO 210 the observed velocity dispersion is ~ 6.5 km s^{-1}and is approximately constant across the galaxy. $\hat{\mathrm{P}}_{\mathrm{HI}}(\vec{U})$ estimated from visibilities averaged across the 10 channels over which the emission has a similar spatial distribution is shown in Fig. 3. Within our measurement

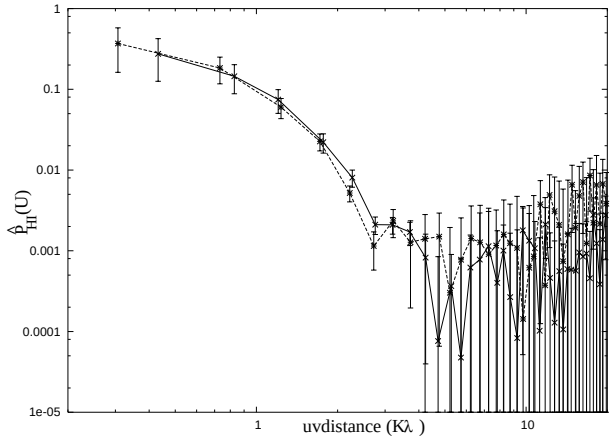

Figure 2. Absolute value of the real part of $\hat{\rm P}_{\rm HI}(\vec{U})$ plotted as a function of uv-distance U for the VLA data (dash line) and the GMRT data (solid line) for a frequency channel with significant HI emission. The GMRT data is exactly the same as in Fig. 1, also the VLA frequency channel has the same heliocentric velocities as the GMRT data.

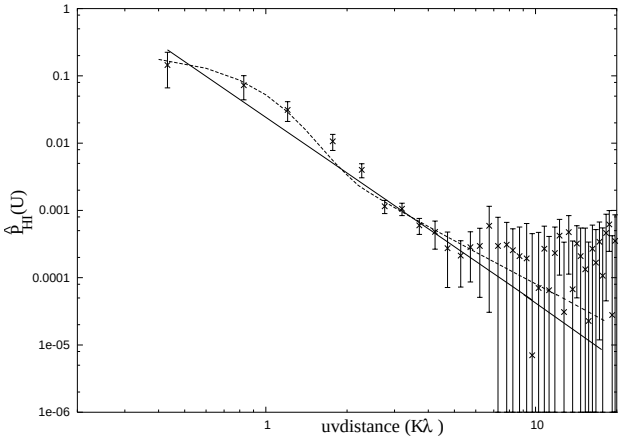

Figure 3. Absolute value of the real part of $\hat{\rm P}_{\rm HI}(\vec{U})$ determined after averaging the GMRT visibilities over the 10 central frequency channels which contain significant HI emission. The best fit power law using the UV range $2 - 12\,{\rm k}\lambda$ is shown as a solid line. The best fit convolved power law over the UV range $0 - 12\,{\rm k}\lambda$ is shown as a dotted line. See the text for more details.

errors, we find no change in the power spectrum with increasing velocity width in the range from ~ 1.7 km s^{-1}to ~ 17 km s^{-1}. We discuss the implications of this in Sec 5, but we note here that in this means that one can work with the emission averaged over channels to improve the signal to noise ratio.

The power spectrum $\hat{\rm P}_{\rm HI}(\vec{U})$ shown in Fig. 3 appears to fall like a power law beyond a uv distance of $\sim 1\,{\rm k}\lambda$. The best fit power law was determined by minimising

$$\chi^2 = \sum_i \frac{[\hat{\rm P}_{\rm HI}(U_i) - AU_i^{\alpha}]^2}{\sigma_i^2} \tag{11}$$

with respect to the amplitude A and the power law index α. It is also necessary to fix the uv range while doing the fit. As can be seen in Fig. 3, $\hat{\rm P}_{\rm HI}(\vec{U})$ flattens below 1 kλ; at these scales one would expect that the convolution with the window function $|\tilde{W}_\nu(\vec{U})|^2$ would be important. If we assume that the convolution with the window function can be ignored for $U > 1$ kλ and do the minimisation described in Eqn. 11 with the lower limit fixed at $U_{\rm min} = 1$ kλ, but several different upper limits $U_{\rm max}$, we find that the minimum χ^2/DOF decreases up to $U_{\rm max} = 12$ kλ but not beyond. For the range $1 - 12$ kλ the best fit power law index is α=$-3.55^{+0.40}_{-0.30}$. Similarly, keeping $U_{\rm min} = 2$ kλ, the best fit power law index for the uv-range $2 - 12$ kλ is α=$-2.85^{+0.50}_{-0.65}$. The best fit for the uv-range $2 - 12$ kλ is shown in Fig. 3. We note that the best fit α is largely determined by the smallest baselines $U \approx U_{\rm min}$ as these have the smallest error bars, and it does not change significantly if $U_{\rm max}$ is changed to say $6\,{\rm k}\lambda$ or even $50\,{\rm k}\lambda$. As one goes to larger and larger baselines however, the minimum in the χ^2 distribution gets more and more shallow – equivalently the error bars on α get larger and larger.

To check the assumption that the convolution with the window function can be ignored for $U > 1$ kλ, we modelled the window function using a Gaussian $\tilde{W}_\nu(\vec{U}) = e^{-U^2/2D^2}$ of width $D = 0.8$ kλ. For a power law form of $\rm P_{HI}(\vec{U})$ we find that the convolution actually produces measurable deviations from the power law at $U \leqslant 2$ kλ. The observed power spectrum is *steeper* than the underlying power law spectrum in the range $1 - 2$ kλ, while at baselines $U \leqslant 1$ kλ it is *flatter* than the underlying power law. We hence repeated the least squares fit to the observed power spectrum using a power law convolved with the assumed Gaussian window function as the input model. For this model the best fit slope for the range $U \leqslant 12$kλ is $\alpha = -2.1^{+0.05}_{-0.10}$. The value of the best fit slope when including baselines < 2kλ could depend on how well the true window function has been modelled. In our analysis we have approximated this with a Gaussian; any deviations from a Gaussian could introduce unknown biases in our estimate of the slope. With this consideration in mind, we also did fits for the restricted uv-range $2 - 12$kλ. For this uv-range, the best fit slope is $\alpha = -2.75 \pm 0.45$. While the fit is good over the fitting range, the model substantially over estimates the power on large scales. This is consistent with the flatter slope (~ -2.1) obtained when fitting over the entire $U \leqslant 12$kλ range, and might be indicative of a deviation from a power law on large scales. However, given the uncertainty in the modelling of the window function it is difficult to make a quantitative statement. On the other hand, our modelling does indicate that beyond about ~ 2kλ the effect of the window function is marginal. The value of the slope obtained after taking into account the convolution (viz. -2.75 ± 0.45) is consistent within the error bars with the value $\alpha = -2.85^{+0.50}_{-0.65}$ obtained without accounting for the convolution. We hence adopt the value $\alpha = -2.75 \pm 0.45$ as slope of the intrinsic power law over these spatial scales.

5 DISCUSSION

Over the uv-range $2 - 12\,{\rm k}\lambda$ (corresponding to spatial scales of 80pc - 500pc) the power spectrum of HI intensity fluctuations in the dwarf galaxy DDO 210 is well described by a power law with slope $\alpha = -2.75 \pm 0.45$. This value is very close to the slope of ~ -3 estimated from the HI emission in our own galaxy (on spatial scales of ~ 5 pc to 200 pc) by Crovisier & Dickey(1983) and Green(1993), and for the SMC (on spatial scales between $\sim$30 pc to 4 kpc; Stanimirovic et al. 1999). The reason why the HI emission power spectrum has a similar slope in the Milky-way as in a galaxy with more than 3 orders of magnitude less HI mass suggests that some fundamental physical process is responsible for determining the power spectrum slope. Power spectral slopes ~ -3 are expected from optically thick turbulent gas

(Lazarian & Pogosyan (2004)). The HI emission from late type dwarfs like DDO 210 is however expected to be optically thin, (see e.g. Haynes & Giovanelli (1984) Giovanelli et al. 1994). Models like those of Goldman (2000) which give a spectral slope ~ -3 in optically thin gas may be more relevant in this case.

Unlike the Milkyway, DDO 210 has no spiral arms and it also has no measurable star formation (van Zee (2000)). The lack of dependence of the power spectrum slope on the star formation rate that we find is similar to the finding of Dib et al. (2006) that the characteristic HI velocity dispersion in galaxies shows a minimum level that is independent of the star formation rate. In this aspect, the turbulence in the gas distribution appears to be different from that in the stellar distribution, where the power spectrum's slope does seem to depend on the star formation rate (Willett 2005). It is possible that the energy source driving the HI turbulence is gravitational energy input on large scales. Detailed simulations suggest that large scale gravitational energy input could explain the substantial turbulent velocity dispersion seen in the outer parts of the extended gas disk of NGC 2915 (Wada et al. (2002)) as well as for the rich structures seen in Holmberg II (Dib & Burket (2005)). Gravitational energy input on large scales (perhaps by tidal torques from other local group members) would also be consistent with the asymmetric large scale HI distribution in DDO 210.

As mentioned in Sec. 4, turbulence produces fluctuations in both the density and velocity fields, in turn, both of these contribute to fluctuations of the HI intensity. Lazarian &Pogosyan (2000) show that the slope of the HI intensity power spectrum goes like $n + \zeta_2/2$ when measured for channel widths that are "thin" compared to the turbulent velocity dispersion, while for channel widths that are "thick" compared to the velocity dispersion the HI intensity power spectrum's slope is n, where n is the slope of the power spectrum of density fluctuations and ζ_2 is the spectral slope of the velocity structure function. Essentially, for velocity widths large compared to the velocity dispersion ("thick" slices) the velocity information gets averaged out and the intensity fluctuations represents density fluctuations. Recall that we find that within the measurement errors the slope of the HI power spectrum does not change for velocity widths ranging from $\sim$ 1.7 km s^{-1}to $\sim$ 17 km s^{-1}. The observed HI velocity dispersion of 6.5 km s^{-1}has contributions from both thermal and turbulent random motions. Our "thick" channel is wider than the total velocity dispersion, and hence we can be sure that the detected power spectrum represents the power spectrum of the HI density fluctuations. Since we get the same slope $\sim -2.75 \pm 0.45$ even for $\sim$ 1.7 km s^{-1}channels, either the turbulence velocity dispersion is smaller than 1.7 km s^{-1}or $\zeta_2 \approx 0 \pm 0.9$. Note that the latter possibility is consistent with $\zeta_2 = 2/3$ which is predicted by the Kolmogorov theory of turbulence.

Acknowledgments The data presented in this paper were obtained using the GMRT (operated by the National Centre for Radio Astrophysics of the Tata Institute of Fundamental Research) and the NRAO VLA. The National Radio Astronomy Observatory is a facility of the US National Science Foundation operated under cooperative agreement by Associated Universities, Inc. SB would also like to acknowledge BRNS, DAE, Govt. of India for financial support through sanction No. 2002/37/25/BRNS.

REFERENCES

Begum, A., & Chengalur, J. N., 2004, A&A, 413, 525
Bharadwaj, S. & Sethi, S. K., 2001, JA&A, 22, 293
Bharadwaj S. & Ali S. S., 2005, MNRAS, 356, 1519
Crovisier, J. & Dickey, J. M., 1983, A&A, 122, 282
Deshpande, A. A., Dwarakanath, K. S., & Goss, W. M., 2000, ApJ, 543, 227
Dib S., Bell, E. & Burkert A., 2006, ApJ, 638, 797.
Dib S. & Burkert A., 2005, ApJ, 630, 238
Elmegreen, B. G., Kim, S. & Staveley-Smith, L., 2001, AJ, 548, 749
Elmegreen B. G. & Scalo J., 2004, ARAA, 42, 211.
Green, D. A., 1993, MNRAS, 262, 327
Hobson, M. P., Lasenby, A. N. & Jones, M., 1995, MNRAS, 275, 863
Lazarian A., Pogosyan D., 2004, ApJ, 616, 943
Lazarian, A. & Pogosyan, D., 2000, ApJ, 537, 720
Lazarian, A., 1995, A&A, 293, 507
Giovanelli R., Haynes M. P., Salzer J. J., Wegner G., da Costa L. N., Freudling W., 1994, AJ, 107, 2036
Goldman I., 2000, ApJ, 541, 701
Haynes M. P., Giovanelli R., 1984, AJ, 89, 758
Lee, M. G., Aparicio, A., Tikonov, N., Byun, Y. & Kim, E., 1999, AJ, 118, 853.
Morales,M. F. and Hewitt,J., 2004, ApJ, 615, 7
Scalo J. & Elmegreen B. G., 2004, ARAA, 42, 275.
Stanimirovic, S., Staveley-Smith, L., Dickey, J. M., Sault, R. J., & Snowden, S. L., 1999, MNRAS, 302, 417
Swarup, G., Ananthakrishnan, S., Kapahi, V. K., Rao, A. P., Subrahmanya, C. R., & Kulkarni, V. K., 1991, Current Science, 60, 95
van Zee L., 2000, AJ, 19 2757
Wada K., Meurer, G. & Norman C. A., 2002, ApJ, 577, 197
Westpfahl, D. J., Coleman, P. H., Jordan, A. & Thomas, T., 1999, AJ, 117, 868
Willett, K. W., Elmegreen, B. G. & Hunter, D. A., 2005, AJ, 129, 2186
Young, L. M., van Zee, L., Lo, K. Y., Dohm-Palmer, R. C. & Beierle, M. E., 2003, ApJ, 592, 111